A Comparison of Structural Steel, Nickel, and Titanium in the Design and Static Structural Finite Element Analysis of a Bladed Rotor-Stator Disc Assembly

KARI BHARATH[1], Mrs. V. SARITHA[2], Dr.B. SANDHYA RANI[3]
[1]PG Student, CAD/CAM, Ellenki College of Engineering and Technology.
[2]Asst. Prof., Department of Mechanical Engineering, Ellenki College of Engineering and Technology.
[3]Head of the Dept. Department of Mechanical Engineering, Ellenki College of Engineering and Technology.

Abstract - Compressors and turbines that use axial flow raise (or, in the case of a turbine, extract) the energy carried by the working fluid and properly redirect its flow between stages. These components are essential in gas-turbine aeroengines, industrial power plants, and large process compression trains. The material choice for the rotors has direct effects on the engine's mass, burst margin, and service life because the rotor blades and discs must endure a substantial centrifugal body load in addition to continuously rotating at high angular speed, something that the stationary stator row never encounters. The central hub, twenty-one aerofoil blades per row generated as multi-section lofts, and a connecting shaft make up a representative two-row, integrally bladed rotor-stator disc. This paper details the solid modeling and static-structural finite element analysis of this disc, and it assesses three potential disc/blade materials: structural steel, commercially pure annealed nickel, and commercially pure Grade-2 titanium, all subjected to the same rotational-acceleration load case. Each material had its own geometry created in CATIA V5 Part Design and then imported into ANSYS Workbench, where a default tetrahedral mesh based on curvature was formed. A rotating acceleration of 10 rad/s² around the shaft axis and a fixed support at the center bore were added to the model. While all three materials experienced relatively small deformations (12.37 mm for structural steel, 13.69 mm for nickel, and 13.45 mm for titanium), the resulting margins of safety were very different. While structural steel and nickel both exceeded their elastic limits under the applied load, titanium maintained a positive margin of safety of about 1.36 with a peak stress of 230.99 MPa against a 315 MPa yield strength. The paper explains that this difference is due to specific strength, which is defined as yield strength divided by density. It then connects this finding to titanium's dominant role in gas turbine compressor rotors and lists the model extensions that are needed to support a certification-oriented conclusion: production-representative alloy grades, steady-state operating-speed loading, thermal effects, and fatigue/resonance assessment.

Index Terms - The following terms are used in this context: axial-flow compressor, rotor-stator assembly, centrifugal loading, von Mises stress, specific strength, margin of safety, and titanium.

I. INTRODUCTION

Each row of rotors performs work on the fluid (or, in the case of a turbine, extracts work from it), while the subsequent row of stators returns the resulting swirling flow to the incidence angle needed by the next row of rotors, in an axial-flow compressor or turbine stage [1, 2]. A whole machine uses many sets of these rotor-stator pairs, with each set adding a little amount of pressure change, to gradually build up the necessary total pressure ratio or power output.

In the same stage, a stator vane and a rotor blade may have equal sizes and aerodynamic characteristics, but their structural surroundings are quite different. The stator vane is typically supported at one or both ends by the fixed housing and experiences solely aerodynamic and thermal stress since it is stationary. While both types of loads are transferred to the disc that supports the rotor blade, the rotor blade experiences a great deal of centrifugal body force when it is placed on a spinning disc. As a result of having to react to both its own inertia and the inward pull of the blades mounted at its rim, the disc bore, which is the surface nearest the shaft, is traditionally where peak hoop and radial stress in such a rotating disc are located, especially at typical operating speeds when this centrifugal component greatly outweighs the gas-bending and thermal contributions [3, 4].

The governing material-selection criterion for a rotating component is specific strength, which is the ratio of strength to density. This stands in stark contrast to the deformation- and stress-concentration-driven trade-offs that usually govern the selection of materials for statically loaded airframe structure. This is due to the fact that centrifugal stress in a spinning disc increases with the square of angular speed and scales linearly with material density. This difference is the driving force for a common load case quantitative direct comparison of potential rotor materials.

For a typical bladed rotor-stator disc setup, this study details such a comparison. The entire geometry, including the hub, two rows of blades, and shaft, was modeled in CATIA V5. Then, three potential materials—structural steel, nickel, and titanium—were subjected to the same rotational acceleration load in a similar ANSYS Workbench static-structural analysis. The goal was to determine and compare the resulting deformation, strain, stress, and margin-of-safety results, and to relate these results to the gas turbine industry's established rotor-material practice.

II. LITERATURE REVIEW

Stage work is connected to the change in swirl velocity by the Euler turbomachinery equation [1, 5], and classical turbomachinery aerodynamics describes each stage via a velocity-triangle description of the flow turning caused by the rotor and then corrected by the stator. According to structural analysis, this aerodynamic loading manifests as a distributed gas-bending stress on both rows of blades. While rotors often experience this loading as a byproduct of centrifugal forces, stator vanes, which do not undergo centrifugal forces themselves, have it as their primary load route [2].

The classical approach to stress in rotating discs, which was initially developed for early flywheel and turbine designs, demonstrates that radial and hoop stresses in a uniformly thick disc change with the square of angular velocity and density, with the maximum stress at the bore for a disc with a central hole [4, 6]. An effect that is acknowledged in production rotor design but is not captured by an integrally bladed idealization, occurs when the extra centrifugal pull of the attached blades is transmitted into the disc rim and concentrates locally at the root fixing when the blades are discretely attached rather than integrally formed with the disc [4].

Applying the finite element approach to rotating structures is a natural progression from its well-established use in static aircraft analysis; the main distinction is in the representation of the centrifugal force. A distributed inertial body force, proportional to the mass of each element and its radial distance from the rotation axis, is introduced as centrifugal loading instead of an externally applied surface pressure or point force. This force is computed by the solver from a specified angular velocity or angular acceleration about a defined axis [7]-[9]. This study distinguishes between the steady-state stress field that would arise from a constant operating speed [8], [9] and the transient inertial loading that is associated with a change of spool speed, such as during rapid throttle application. The former is called a rotational-acceleration load.

Historically, structural steel has been used as a possible rotor material when operating temperature and specific-strength requirements did not need a more specialized alloy [10]. It is a well-characterized and widely-available metallic basis. Due to their creep resistance and ability to retain high temperatures, nickel-based alloys find widespread application in gas turbine engine hot sections. However, the production discs and blades made of precipitation-hardened, multi-element superalloys have much higher room-temperature and elevated-temperature strengths than the bounding reference case of unalloyed nickel [11]. For compressor rotor discs and blades, titanium alloys are the material family of choice because they have a good balance of specific strength, fatigue resistance, and sufficient strength retention up to the moderate temperatures encountered in the compressor section [10], [11].

Compressor and turbine blade and disc modeling in CATIA V5 is common because the program's surface and multi-section lofting tools work well with the twisted, spanwise-varying aerofoil geometry seen in turbomachinery blading, and the program's circular-pattern capability makes it possible to create a full row of evenly spaced blades from a single parent profile [12], [13]. The special contribution of this research is a like-for-like comparison of an unalloyed structural-steel, nickel, and titanium rotor-stator assembly under an identical rotational-acceleration stress situation. No study found in the current review provides this compares at a similar level of detail.

III. METHODOLOGY

A. Design Details and Parts Catalogue

The part being studied is a two-row rotor-statator disc with simplified, integrally bladed design. It has a central hub and shaft interface and two rows of aerofoil blades around the disc, with each row being made up of a complete 360° pattern of a single lofted blade profile. The study's primary geometry and load parameters are summarized in Table I.

Design and Load Parameters for Rotor-Stator Combinations (Table I)

Parameter	Value / Description
Overall assembly length	≈ 1,050 mm (representative sub-scale two-stage assembly)
Number of blade rows	2 (rotor and stator stage pair)
Blades per row	21 (circular-pattern instances, 17.143° spacing)
Blade construction	Multi-section solid loft between root and tip aerofoil sections
Central bore / shaft	Fixed-support boundary condition
Applied load	Rotational acceleration of 10 rad/s² about the shaft axis

The hub served as the foundation and reference geometry for the subsequent rows of blades; it was constructed as a pad feature that was extruded from a rotationally symmetrical contour. Then, for every row of blades, we placed planes at the hub surface and the design span radius to sketch the root and tip aerofoil sections, lofted a single blade solid between them, and used a circular-pattern operation around the assembly's rotational axis to create 21 evenly spaced instances that made up a full crown. A revolving shaft was used to link the two bladed hub pieces and finish the load passage between rows after the second (stator) row was built using the same loft-and-pattern sequence at the correct axial offset.

B. Supply items

In order to facilitate a direct, like-for-like structural comparison, three candidate materials were assigned to the rotor-stator geometry in separate analyses. These materials were structural steel, which represents a conventional metallic baseline; commercially pure, annealed nickel, which represents the nickel-based alloy family used in hot-section turbomachinery in bounding, unalloyed form; and commercially pure, Grade-2 titanium, which represents the titanium alloy family used extensively in compressor rotor applications in bounding, unalloyed form. The mechanical properties of each material are listed in Table II, which is sourced from the ANSYS Engineering Data / Granta Design library. It is anticipated that the materials that stay within their elastic range under the applied centrifugal load are nickel and structural steel, since the latter two have a lower yield strength than titanium and the former also has the highest density.

The table Part II: Materials and Mechanical Characteristics of Potential Rotor-Stators

Property	Structural Steel	Nickel (Comm. Purity)	Titanium (Grade 2)
Density (kg/mm³)	7.85×10^{-6}	8.9×10^{-6}	4.51×10^{-6}
Young's Modulus (MPa)	200,000	204,000	102,000
Poisson's Ratio	0.30	0.31	0.36
Tensile Yield Strength (MPa)	250	150	315
Tensile Ultimate Strength (MPa)	460	456	411

C. Finite Element Modeling and Solid Modeling

With the help of an associative specification tree in the model, any changes made to the parent blade profile will automatically be reflected in all 21 patterned instances in each row. The entire rotor-stator geometry was created as a single CATIA V5 Part Design solid, following a sketch-driven, feature-based sequence that included operations such as pad, multi-section solid loft, circular pattern, and shaft (revolve). By using CATIA's native ANSYS geometry interface, the completed component was imported into the ANSYS Workbench project schematic from the original CATPart format, with the solid body and named bore face necessary for the boundary condition preserved.

The imported geometry was subjected to the three candidate materials listed in Table II in ANSYS Workbench. The geometry was then meshed using the default automatic mesh generator, which takes into account both curvature and proximity. The result was a mixed tetrahedral mesh that covered the hub, both rows of blades, and the shaft. Automatic local refinement was applied at the leading and trailing edges of the blades, as well as at the fillets connecting the hub and blades, where the surface curvature was found to be the highest. At the center bore of the assembly, a fixed-support boundary condition was applied to mimic the constraint that the shaft coupling and bearing structure would provide in an actual engine installation. On the other hand, the shaft axis was subjected to a rotational acceleration of 10 rad/s² to simulate a temporary change in speed rather than the steady-state stress field linked to a constant operating speed. For each material, we independently updated the Engineering Data assignment and re-solved to get the resultant linear-elastic static structural solution. This allowed us to compare the three situations like for like.

The ANSYS Mechanical result summary was used to extract deformation, elastic strain, and equivalent (von Mises) stress from each material. These were then compared to the corresponding tensile yield strength from Table II to determine a margin of safety. The component mass, which was calculated from the constant assembly volume and each material's density, was recorded alongside the structural results to support the discussion of specific-strength trade-offs in Section V.

IV. RESULTS

Under the common rotational-acceleration load example, this section gives the three candidate materials' total deformation, equivalent elastic strain, and equivalent (von Mises) stress, as well as the consequent margin of safety and relative component mass.

A. Overall Deformity

Structure steel had a maximum total deformation of 12.37 mm, nickel of 13.69 mm, and titanium of 13.45 mm. Given that titanium has a density three times lower than the other two candidates, the applied load scales with density. Since the centrifugal body force driving deformation is directly proportional to mass, titanium's density reduces the applied load in a ratio of its stiffness to its density, effectively canceling out the deformation penalty caused by its lower Young's modulus. Consequently, all three results fall into a relatively narrow band. Of the three, nickel has the slightest advantage in peak deformation due to its somewhat greater density and stiffness compared to steel.

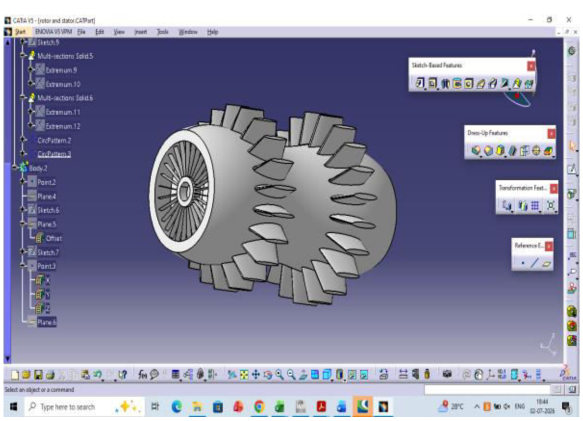

Figure 1: The rotor-stator edge assembly in CATIA V5, with the hub in the center, two rows of blades around the circumference, and the interface between the two shafts.

B. The Elastic Strain That Works

Concentrating on the hub-to-blade fillet and root areas, the maximum equivalent elastic strain coordinates with the stress field, as shown below, for all materials. The structural steel, nickel, and titanium peak values were 2.1049×10^{-3} mm/mm, 2.33×10^{-3} mm/mm, and 2.307×10^{-3} mm/mm, respectively. These values are in agreement with the peak stress and elastic modulus of the respective materials, and they prove that the solution for all three materials is contained within the linear-elastic solver formulation that was used.

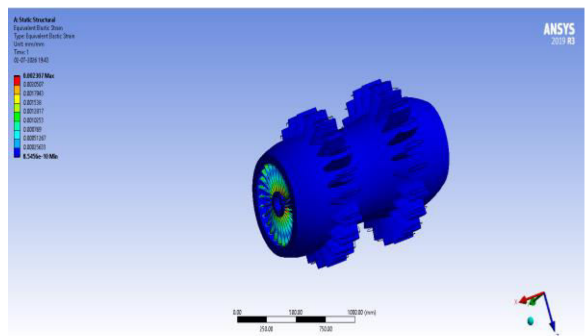

Figure 2. Titanium rotor-stator assembly (equivalent elastic strain contour, maximum 2.307×10^{-3} mm/mm)

C. Stress and Safety Margin That Are Equivalent to von Mises

Where the inertia of the spinning disc meets the inward centrifugal force communicated by the blades, the hub/blade-root fillet area saw peak equivalent stresses of 416.34 MPa for structural steel, 469.24 MPa for nickel, and 230.99 MPa for titanium. Table II shows that when we compare the peak values to the tensile yield strengths of the materials, we find that structural steel has a margin of safety of 0.60 and nickel has a margin of safety of 0.32. This means that both of these materials are predicted to experience local yielding under the applied rotational-acceleration load. In contrast, titanium has a margin of safety of about 1.36, making it the only candidate out of the three that stays within its elastic range under the applied load.

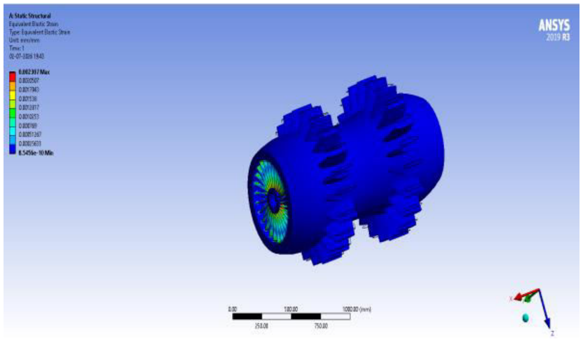

Figure 3. Titanium rotor-stator assembly (equivalent elastic strain contour, maximum 2.307 × 10^{-3} mm/mm)

D. Overview of Similar

Table III summarizes the relative mass, deformation, stress, and margin-of-safety values for the three potential materials. Among the three contenders, titanium has the lowest component mass and the only positive margin of safety (about 57.5% of the structural-steel baseline), whereas nickel has the highest mass and the worst margin of safety (the worst outcome on both counts at once).

The table I. Summary of Results from Finite Element Analysis III.

Material	Max. Deformation (mm)	Max. Equiv. Stress (MPa)	Margin of Safety	Relative Mass (% of Steel)
Structural Steel	12.37	416.34	0.60	100%
Nickel	13.69	469.24	0.32	≈ 113.4%
Titanium	13.45	230.99	1.36	≈ 57.5%

V. DISCUSSION

When comparing materials for statically loaded airplane construction, any plausible choice usually stays structurally viable to some degree. However, the pattern of findings revealed here departs significantly from that. Titanium has a healthy safety margin compared to structural steel and nickel, which are both expected to surpass their yield strength when subjected to the same load. The results here are quite clear-cut. Because the resistance to centrifugal stress is yield strength and centrifugal stress scales with density, the specific strength of a material (yield strength divided by density) becomes the first-order predictor of rotor structural viability. This binary split is a direct result of the centrifugal-loading regime described in Section II. Out of the three contenders, titanium has the lowest density (4.51 × 10^{-6}) and the highest yield strength (315 MPa). Its specific strength is about 4.2 times higher than the unalloyed nickel tested here and around 2.6 times higher than structural steel (kg/mm³).

It should also be noted that the applied load is a rotational acceleration and not a steady-state operating speed. All three materials were subjected to the same 10 rad/s² angular acceleration on the same geometry, so the resulting stress fields are directly comparable. However, these stress fields should not be interpreted as representing the continuous, steady-state centrifugal stress field that the assembly would experience at a specific certification-relevant operating speed.

Titanium has long been the material of choice for gas turbine compressor rotors, and its obvious structural advantage both supports and provides a reason for this supremacy. The yield strength of the unalloyed nickel used in this study is 150 MPa, which is significantly lower than the precipitation-hardened superalloys used in production turbine rotors. These rotors achieve much higher room- and elevated-temperature strengths. This difference is fundamental to the industry's traditional division of labor between nickel-superalloy turbine rotors and titanium compressor rotors, since titanium alloys cannot replace nickel superalloys in the hotter turbine section due to their own oxidation and creep behavior, which limits them to temperatures around 550-600 °C.

There is a self-reinforcing advantage to using titanium in rotating structures, which is a large mass reduction (about 42.5% below the structural-steel baseline). This is because a lower density lowers the component's weight and, because the applied load is density-proportional, reduces the internal stress the material must withstand. This effect is not seen in statically loaded structures, where stress is typically independent of the material's density.

While trying to make sense of these findings, keep in mind a few caveats. The properties of the nickel and titanium used are those of commercially pure, unalloyed reference materials, not of the precipitation-hardened superalloys and alpha-beta titanium alloys used in production rotors (like Ti-6Al-4V). Therefore, the absolute margin-of-safety values should be interpreted as showing trends across material families, not as being directly applicable to a particular production alloy. The measured peak stresses probably understate those of a discrete-attachment rotor with similar overall geometry since the integrally bladed geometry does not account for the locally concentrated stress that would be introduced by a discrete firtree or dovetail blade-root attachment in a production design. Not included in this static, single-load-case study are the following: the rotational-acceleration load case, which is more of a transitory state than a specific, certification-relevant continuous operating speed; thermal loading, which is more relevant to turbine stages than compressor stages; low- and high-cycle fatigue; and Campbell-diagram resonance assessment.

VI. CONCLUSION

Under a fixed support at the central bore and a rotational acceleration of 10 rad/s² about the shaft axis, a two-row, integrally bladed rotor-stator disc modeled in CATIA V5 and run through an identical ANSYS Workbench static-structural finite element analysis were three candidate materials: structural steel, nickel, and titanium. The disc consists of a central hub, two rows of twenty-one blades generated by a multi-section loft and a circular pattern, and a connecting shaft. Although all three materials experienced relatively small deformation, the resulting margin of safety varied greatly. Titanium (1.36), having the lowest component mass of the three candidates, stayed within its elastic range, while structural steel (0.60) and nickel (0.32) were expected to surpass their elastic limit when subjected to the applied load. The outcome provides a quantitative, first-principles explanation for titanium's long-standing supremacy as a material for gas-turbine compressor rotors, and it is ascribed to the specific-strength-driven character of centrifugally loaded rotating structures, where density is a first-order design variable, as opposed to statically loaded structures. For a given rotor material and geometry combination, the model needs to be extended to include production-representative alloy grades, steady-state operating-speed loading, thermal loading, fatigue and resonance assessment, and other specifics before it can support a certification-level conclusion.

REFERENCES

[1] Rolls-Royce plc, The Jet Engine, 5th ed. Derby, U.K.: Rolls-Royce plc, 1996.

[2] H. I. H. Saravanamuttoo, G. F. C. Rogers, H. Cohen, and P. V. Straznicky, Gas Turbine Theory, 6th ed. Harlow, U.K.: Pearson, 2009.

[3] M. P. Boyce, Gas Turbine Engineering Handbook, 4th ed. Oxford, U.K.: Butterworth-Heinemann, 2011.

[4] S. P. Timoshenko and J. N. Goodier, Theory of Elasticity, 3rd ed. New York, NY: McGraw-Hill, 1970.

[5] L. Reid and R. D. Moore, "Design and overall performance of four highly loaded, high-speed inlet stages for an advanced high-pressure-ratio compressor," NASA Technical Paper 1337, 1978.

[6] M. C. Y. Niu, Airframe Structural Design: Practical Design Information and Data on Aircraft Structures, 2nd ed. Hong Kong: Conmilit Press, 1999.

[7] O. C. Zienkiewicz, R. L. Taylor, and J. Z. Zhu, The Finite Element Method: Its Basis and Fundamentals, 7th ed. Oxford, U.K.: Butterworth-Heinemann, 2013.

[8] ANSYS, Inc., ANSYS Mechanical User's Guide, Release 2019 R3. Canonsburg, PA: ANSYS, Inc., 2019.

[9] ANSYS, Inc., ANSYS Mechanical APDL Structural Analysis Guide, Release 2019 R3. Canonsburg, PA: ANSYS, Inc., 2019.

[10] M. J. Donachie, Titanium: A Technical Guide, 2nd ed. Materials Park, OH: ASM International, 2000.

[11] R. C. Reed, The Superalloys: Fundamentals and Applications. Cambridge, U.K.: Cambridge University Press, 2006.

[12] Dassault Systèmes, CATIA V5 Part Design User Guide. Vélizy-Villacoublay, France: Dassault Systèmes, 2020.

[13] ASM International, ASM Handbook, Volume 2: Properties and Selection: Nonferrous Alloys and Special-Purpose Materials. Materials Park, OH: ASM International, 1990.